Kinematics and Design of a Wheeled Mobile Robot

December, 2002

Fan Tang

Centre for Intelligent Machines, McGill University,

Montreal, Quebec, H3A 2K6, Canada

Centre for Intelligent Machines (CIM) and

Department of Mechanical Engineering

McGill University, Montreal, Quebec, Canada

Abstract

We report on the kinematics of a wheeled mobile robot (WMR) with three dual-wheel transmission (DWT) units. Design parameters of DWT units of the WMR are chosen under the criteria of kinetostatic robustness and practical design. In addition, the mobility of the robot with three dual-wheel mechanisms is investigated. Finally, the complete design, up to the manufacturing drawings, of the whole mechanical system is also reported here.

1 Introduction

As highly automated manufacturing processes with lower costs are required by industry, the efficient transportation of materials, parts and sub-assemblies is needed to be able to deliver just-in-time. In fact, automated guided vehicles (AGVs) have been broadly used in industry. As their guidance mechanism is very expensive to alter, AGVs are no longer suited for such a dynamic manufacturing environment. Under these circumstances, innovative mobile robots which can manoeuvre efficiently in these environments are needed. There are collectively known as wheeled mobile robots, abbreviated WMRs.

Currently, besides limited applications of some industrial and commercial robots, applications of WMR have pervaded many other fields. Examples are shown in Fig. 1. Mobile robots come in many shapes. These include legged, treaded and wheeled robots [1]. By far, wheeled mobile robots are the best suited for industrial environments. Compared with their legged and treaded counterparts, WMR offer an excellent balance regarding load-carrying capacity, manoeuvrability and low operation and maintainance costs. However, wheels have a tendency to be bogged on uneven and soft terrain. As most of factory floors are typically smooth, flat and hard, wheeled mobile robots are ideally suited for manufacturing applications.

The types of robot wheels are defined by Muir and Neuman [1] as conventional, omnidirectional and ball-wheels. Recently, some other types of wheel mechanism for WMR

(a) (b)

Figure 1: Examples of applications for mobile robots: (a) wheelchair for the disabled; (b) a cleaning robot

have been reported, such as the dual-wheel transmission [2], the dual-wheel caster drive [3], orthogonal wheels [4] and double-wheel drives [5]. The R&D of mobile robots targets five different areas, namely, locomotion, manipulation sensing, communication and reasoning. The first area, locomotion, covers robot kinematis and dynamics, transmission design, power management, motion control and electromechanical integration. This project focuses on the kinematics and design of wheeled mobile robots with three dual-wheel transmission.

2 Kinematic Modelling and Analysis of the Dual-Wheel Transmission

2.1 Generalities

Conventional wheels are by far the most widely used among WMRs with wheeled locomotion. Conventional wheels come in two types, namely, centred and offset wheels, as shown in Figs. 2a and 2b, respectively. Both types, when mounted on a vertical steerable

(a) (b)

Figure 2: Examples of conventional wheels: (a) centred; (b) offset

axis, have two degrees of freedom. In the first type, the centre lies at the intersection of the axes of rolling and steering. In the second type, also known as caster wheels, the axis of steering is offset from the axis of rolling. The kinematic analysis of the above two different wheels was reported by Leow [2].

To drive offset or centred wheels, two actuators are needed to provide the steering and

rolling motions. The steering actuator calls for position control, while the driving actuator for velocity control. Therefore, two independent control systems are required, which can lead to problems of coordination and synchronization. Other practical problems can also arise because the two types of actuators may not be available from the same manufacturer. The dual-wheel transmission (DWT), in which wheels are driven by two identical independent actuators, is aimed at solving the foregoing problems. The steering of the DWT is done by the two wheels when turning at different rates. Therefore, the two wheels are governed by identical control systems, which can be safely coordinated and synchronized to provide both position and velocity accuracy.

The kinematic analysis of the dual-wheel transmission is outlined in the balance of the section.

2.2 Kinematics of the Dual-Wheel Transmission

The dual-wheel transmission comprises two epicyclic gear mechanisms coupled by a common planet carrier, as depicted in Fig. 3. For analysis purposes, the motor-carrier is taken as the reference body, and hence, numbered 0. The sun gear 1 of the upper train is rigidly mounted on the hollow shaft of gear 7, which is coupled by means of a pinion, coupled, in turn, to motor M by means of a pinion 6. The sun gear 4 of the lower train is rigidly mounted on the solid shaft of gear $7'$, which is coupled by means of a pinion $6'$ to motor M'. The planet 3 is rigidly mounted on the cardan shaft $8'$, which turns at

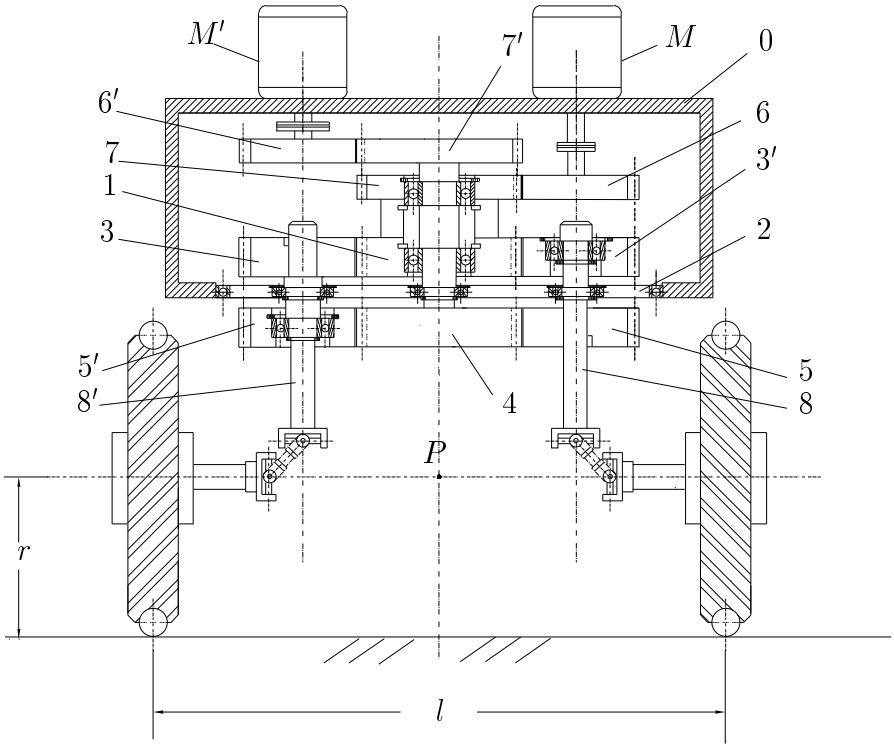

Figure 3: Conceptual layout of the dual-wheel transmission

the same rate as the planet gear. Planet $3'$, its companion, is traversed by the cardan shaft 8, to which it is articulated by means of bearings. Thus, gear $3'$ is free to rotate about shaft 8. Similarly, planet 5 is rigidly mounted on the cardan shaft 8, which turns at the same rate as this planet. Planet $5'$, its companion, is traversed by the shaft $8'$, to which it is articulated by means of bearings. Thus, gear $5'$ is free to rotate about shaft $8'$. Torque and motion are transmitted from the two shafts 8 and $8'$ to the two wheels via an array of universal joints with angles of $45°$. The two epicyclic trains share

a common planet carrier denoted by 2. The motors are rigidly mounted on the platform of the WMR, denoted by 0 in Fig. 3. The whole mechanism can rotate freely by means of bearings with respect to the platform. This setup has the advantage of keeping the motors fixed to the body and prevent the entangling of electrical cables.

Obviously, this transmission is not a direct drive; therefore, the relations between the motor output velocities and the wheel, the planet carrier and the platform output velocities have to be established.

The notation used in deriving the kinematic relations are described below:

N_i: number of teeth of gear i, for $i = 1, 3, 5, 6, 7, 8, 9, 10$ with $N_{3'} = N_3$ and $N_{5'} = N_5$.

ω_i: angular velocity of the ith rotating element with respect to the ground.

ω_i': angular velocity of the ith rotating element with respect to the planet carrier 2.

ω_i'': angular velocity of the ith rotating element with respect to the platform 0.

l: distance between the wheel-ground contact points.

r: radius of the wheels.

$\rho = r/l$: the ratio of the wheel radius to the distance between contact points.

Although not necessary, it is highly recommended that the design be made symmetrical by selecting the same number of teeth for gears 1, 4, 7 and 7′, and for 3, 5, 6 and 6′, such that $N_1 = N_4 = N_7 = N_{7'}$ and $N_3 = N_5 = N_6 = N_{6'}$.

Furthermore, let us define γ as the gear ratio between gears 3 and 1. Apparently, the motion inputs ω_6 and $\omega_{6'}$ are the motor angular velocities with respect to the platform 0. The wheel outputs are, in fact, the angular velocities of the planets 3 and 5 with respect to the planet carrier 2. Thus, the sun gear 1, the planet 6 and the platform 0 form an epicyclic gear train. The kinematic relations for this train are well known [6]. In our case, these relations take the form

$$\frac{\omega_1 - \omega_0}{\omega_6 - \omega_0} = -\frac{N_6}{N_1} = -\gamma \tag{1}$$

A similar relation, but using velocities with respect to the planet carrier 2, readily follows:

$$\frac{\omega_1' - \omega_0'}{\omega_6' - \omega_0'} = -\frac{N_6}{N_1} = -\gamma \tag{2}$$

Equation (2) can be rewritten as

$$\omega_1' = (1+\gamma)\omega_0' - \gamma\omega_6' \tag{3}$$

We also have

$$\omega_0' = \omega_0 - \omega_2, \qquad \omega_6' = \omega_6'' + \omega_0 - \omega_2 \tag{4}$$

Equation (3) can be rewritten as

$$\omega_1' = \omega_0 - \omega_2 - \gamma\omega_6'' \tag{5}$$

Likewise,

$$\omega_4' = \omega_0 - \omega_2 - \gamma\omega_{6'}'' \tag{6}$$

Moreover,

$$\omega_1' = -\gamma\omega_3', \qquad \omega_4' = -\gamma\omega_5' \tag{7}$$

We substitute now eq.(7) into eqs.(5) and (6) to obtain

$$\omega_3' = \omega_6'' - \frac{1}{\gamma}(\omega_0 - \omega_2) \tag{8}$$

Likewise,

$$\omega_5' = \omega_{6'}'' - \frac{1}{\gamma}(\omega_0 - \omega_2) \tag{9}$$

Notice that the absolute angular velocity of each wheel is identical to the relative velocity of its corresponding planet with respect to the planet carrier 2, rather than to the absolute velocity of that planet. Furthermore, under the assumption that the two wheels roll without slipping, the angular velocity ω_2 can be expressed as

$$\omega_2 = \frac{r}{l}(\omega_3' + \omega_5') = \rho(\omega_3' + \omega_5') \tag{10}$$

The velocity v of P, the midpoint of the wheel-axle shown in Fig. 3, can be expressed, in turn, as

$$v = \frac{r}{2}(\omega_3' - \omega_5') \tag{11}$$

where we have defined ρ as $\rho = r/l$. Below we cast eqs.(8), (9), (10) and (11) in dimensionally-homogeneous form:

$$\omega_6'' = \frac{1}{\gamma}\omega_0 + \left(\frac{1}{2\rho} - \frac{1}{\gamma}\right)\omega_2 + \frac{v}{r} \tag{12a}$$

$$\omega_{6'}'' = \frac{1}{\gamma}\omega_0 + \left(\frac{1}{2\rho} - \frac{1}{\gamma}\right)\omega_2 - \frac{v}{r} \tag{12b}$$

$$\omega_3' = \frac{\omega_2}{2\rho} + \frac{v}{r} \tag{12c}$$

$$\omega_5' = \frac{\omega_2}{2\rho} - \frac{v}{r} \tag{12d}$$

We have thus introduced seven variables, including six angular velocities, namely, ω_2, ω_3', ω_0, ω_5', ω_6'', $\omega_{6'}''$ plus one translational velocity, v. If the values of ω_2, ω_0 and v are given, then we can solve for the remaining four unknowns ω_3', ω_5', ω_6'', $\omega_{6'}''$ by means of the constraints, eqs.(8), (9), (10), (11), thereby completing the kinematic analysis of the dual-wheel transmission.

3 Kinematics of a WMR with Three DWT Units

3.1 Platform Kinematics

A WMR consists of N wheels and a platform, which is supported by the former, as shown in Fig. 4. A WMR can be designed with any type of wheel, centred, offset or dual, or a combination thereof. The motion of the platform can be described by one orientation and two translations in the **i** and **j** directions, the associated velocities being grouped in the *twist* vector [7] $\mathbf{t}_p = [\dot{\psi} \quad \dot{\mathbf{c}}^T]^T$, with the notation shown in Fig. 5. In this figure, $\dot{\psi}$ is the angular velocity of frame $\mathcal{A}$ rotating with respect to the fixed reference frame $\mathcal{F}$ about a vertical axis; $\dot{\mathbf{c}}$ is the two-dimensional velocity vector of the platform centre C. Moreover, we define $\|\mathbf{d}_j\| = d$, which is the magnitude of $\mathbf{d}_j$.

The absolute velocity of a point P_j of the platform, of position vector $\mathbf{p}_j$, can be obtained

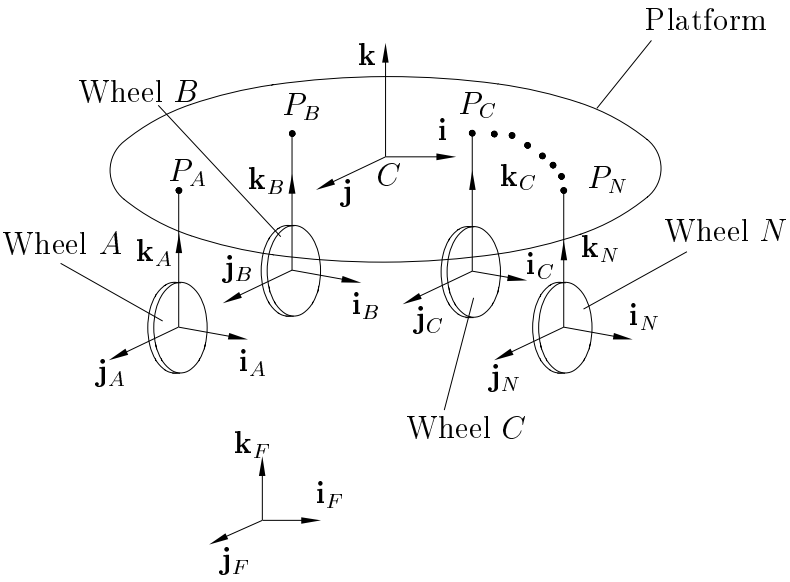

Figure 4: Layout of a generic WMR

as

$$\dot{\mathbf{p}}_j = \dot{\mathbf{c}} + \dot{\psi}\mathbf{E}\mathbf{d}_j, \quad j = A, B, \ldots, N \tag{13}$$

where $\mathbf{E}$ is a 2×2 skew-symmetric matrix, namely [7],

$$\mathbf{E} = \begin{bmatrix} 0 & -1 \\ 1 & 0 \end{bmatrix} \tag{14}$$

and $\mathbf{d}_j$ is the vector directed from C to P_j, for $j = A$, B,..., N. Moreover, we define vector $\mathbf{h}_j$ as

$$\mathbf{h}_j = \mathbf{E}\mathbf{d}_j \tag{15}$$

Equation (13) can now be rewritten as

$$\dot{\mathbf{p}}_j = \dot{\mathbf{c}} + \dot{\psi}\mathbf{h}_j \tag{16}$$

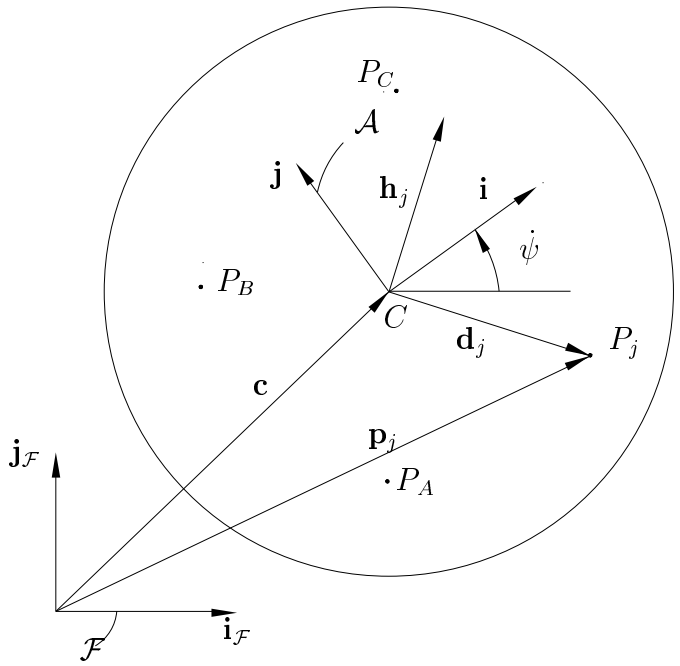

Figure 5: Notation for the platform motion

or

$$\dot{\mathbf{p}}_j = \mathbf{P}_j \mathbf{t}_p \tag{17a}$$

where $\mathbf{P}_j$ is a 2×3 matrix and $\mathbf{t}_p$ is the three-dimensional *twist* of the platform, namely,

$$\mathbf{P}_j = \begin{bmatrix} \mathbf{h}_j & \mathbf{1} \end{bmatrix}, \qquad \mathbf{t}_p = \begin{bmatrix} \dot{\psi} \\ \dot{\mathbf{c}} \end{bmatrix} \tag{17b}$$

thereby completing the kinematic analysis of the platform of the WMR.

3.2 Kinematic Analysis of the WMR

In formulating the kinematic analysis of the WMR, we introduce some assumptions that will simplify the analysis. We assume that the WMR is composed of rigid bodies connected by ideal joints; it operates on a flat horizontal surface free of obstacles; the friction at the contact points between wheel and ground is large enough to prevent slippage; and the wheels can be modelled as thin disks.

Moreover, the simplified architecture of the dual-wheel transmission is shown in Fig. 6, where j represents the jth dual-wheel transmission of the WMR.

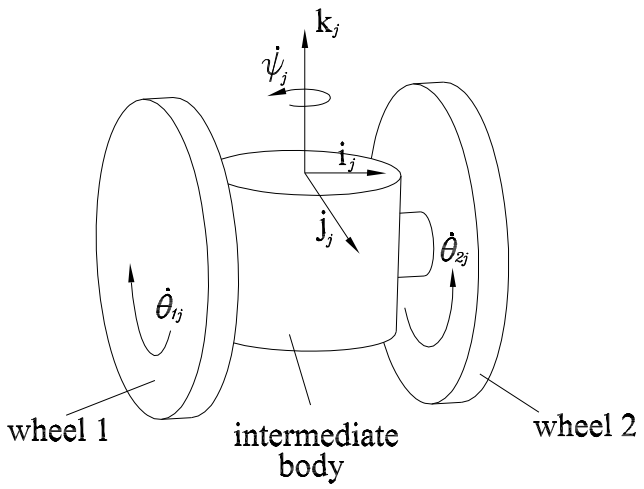

Figure 6: Simplified architecture of the dual-wheel transmission

We now study the WMR with three dual-wheel transmission units, which are denoted

A, B and C, respectively. We define, moreover,

$$\dot{\psi} = \omega_0 \tag{18}$$

For unit A,

$$\dot{\psi_A} = \omega_{2A}, \qquad \dot{\theta}_{A1} = \omega'_{3A}, \qquad \dot{\theta}_{A2} = \omega'_{5A} \tag{19}$$

For unit B,

$$\dot{\psi_B} = \omega_{2B}, \qquad \dot{\theta}_{B1} = \omega'_{3B}, \qquad \dot{\theta}_{B2} = \omega'_{5B} \tag{20}$$

For unit C,

$$\dot{\psi_C} = \omega_{2C}, \qquad \dot{\theta}_{C1} = \omega'_{3C}, \qquad \dot{\theta}_{C2} = \omega'_{5C} \tag{21}$$

Further, we define the motor output velocities as the input variables of the dual-wheel transmission, the angular velocity of each DWT unit and the twist of the platform as the output variables of the system. The Jacobian matrix relating the input with the output variables is to be derived.

Equations (8) and (9), for unit A, can be rearranged as

$$\dot{\theta}_{A1} = \omega''_{6A} - \frac{1}{\gamma}(\dot{\psi} - \dot{\psi}_A) \tag{22a}$$

$$\dot{\theta}_{A2} = \omega''_{6'A} - \frac{1}{\gamma}(\dot{\psi} - \dot{\psi}_A) \tag{22b}$$

For unit B, in turn,

$$\dot{\theta}_{B1} = \omega''_{6B} - \frac{1}{\gamma}(\dot{\psi} - \dot{\psi}_B) \tag{23a}$$

$$\dot{\theta}_{B2} = \omega''_{6'B} - \frac{1}{\gamma}(\dot{\psi} - \dot{\psi}_B) \tag{23b}$$

while, for unit C,

$$\dot{\theta}_{C1} = \omega''_{6C} - \frac{1}{\gamma}(\dot{\psi} - \dot{\psi}_C) \tag{24a}$$

$$\dot{\theta}_{C2} = \omega''_{6'C} - \frac{1}{\gamma}(\dot{\psi} - \dot{\psi}_C) \tag{24b}$$

The non-slipping conditions thus lead to three kinematic constraints for the DWT.

For DWT A,

$$\dot{\psi}_A = \frac{r}{l}(\dot{\theta}_{A1} + \dot{\theta}_{A2}) = \rho(\dot{\theta}_{A1} + \dot{\theta}_{A2}) \tag{25a}$$

$$\dot{\mathbf{p}}_A = \frac{r}{2}(\dot{\theta}_{A1} - \dot{\theta}_{A2})\mathbf{j}_A \tag{25b}$$

For DWT B,

$$\dot{\psi}_B = \frac{r}{l}(\dot{\theta}_{B1} + \dot{\theta}_{B2}) = \rho(\dot{\theta}_{B1} + \dot{\theta}_{B2}) \tag{26a}$$

$$\dot{\mathbf{p}}_B = \frac{r}{2}(\dot{\theta}_{B1} - \dot{\theta}_{B2})\mathbf{j}_B \tag{26b}$$

For DWT C,

$$\dot{\psi}_C = \frac{r}{l}(\dot{\theta}_{C1} + \dot{\theta}_{C2}) = \rho(\dot{\theta}_{C1} + \dot{\theta}_{C2}) \tag{27a}$$

$$\dot{\mathbf{p}}_C = \frac{r}{2}(\dot{\theta}_{C1} - \dot{\theta}_{C2})\mathbf{j}_C \tag{27b}$$

From eq.(16), we can obtain

$$\dot{\mathbf{p}}_A = \dot{\mathbf{c}} + \dot{\psi}\mathbf{h}_A \tag{28a}$$

$$\dot{\mathbf{p}}_B = \dot{\mathbf{c}} + \dot{\psi}\mathbf{h}_B \tag{28b}$$

$$\dot{\mathbf{p}}_C = \dot{\mathbf{c}} + \dot{\psi}\mathbf{h}_C \tag{28c}$$

Combining eqs.(28a), (28b), (28c) with eqs.(25b), (26b), (27b), we obtain

$$\dot{\mathbf{c}} + \dot{\psi}\mathbf{h}_A = \frac{r}{2}(\dot{\theta}_{A1} - \dot{\theta}_{A2})\mathbf{j}_A \tag{29a}$$

$$\dot{\mathbf{c}} + \dot{\psi}\mathbf{h}_B = \frac{r}{2}(\dot{\theta}_{B1} - \dot{\theta}_{B2})\mathbf{j}_B \tag{29b}$$

$$\dot{\mathbf{c}} + \dot{\psi}\mathbf{h}_C = \frac{r}{2}(\dot{\theta}_{C1} - \dot{\theta}_{C2})\mathbf{j}_C \tag{29c}$$

Substracting eq.(22a) from eq.(22b), (23a) from (23b) and (24a) from (24b) leads to

$$\dot{\theta}_{A1} - \dot{\theta}_{A2} = \omega''_{6A} - \omega''_{6'A} \tag{30a}$$

$$\dot{\theta}_{B1} - \dot{\theta}_{B2} = \omega''_{6B} - \omega''_{6'B} \tag{30b}$$

$$\dot{\theta}_{C1} - \dot{\theta}_{C2} = \omega''_{6C} - \omega''_{6'C} \tag{30c}$$

Substituting eqs.(30a), (30b), (30c) into eqs.(29a), (29b), (29c) yields

$$\dot{\mathbf{c}} + \dot{\psi}\mathbf{h}_A = \frac{r}{2}(\omega''_{6A} - \omega''_{6'A})\mathbf{j}_A \tag{31a}$$

$$\dot{\mathbf{c}} + \dot{\psi}\mathbf{h}_B = \frac{r}{2}(\omega''_{6B} - \omega''_{6'B})\mathbf{j}_B \tag{31b}$$

$$\dot{\mathbf{c}} + \dot{\psi}\mathbf{h}_C = \frac{r}{2}(\omega''_{6C} - \omega''_{6'C})\mathbf{j}_C \tag{31c}$$

Adding eq.(22a) to (22b), (23a) to (23b), and (24a) to (24b), we obtain, moreover,

$$\dot{\theta}_{A1} + \dot{\theta}_{A2} = \omega''_{6A} + \omega''_{6'A} - \frac{2}{\gamma}(\dot{\psi} - \dot{\psi}_A) \tag{32a}$$

$$\dot{\theta}_{B1} + \dot{\theta}_{B2} = \omega''_{6B} + \omega''_{6'B} - \frac{2}{\gamma}(\dot{\psi} - \dot{\psi}_B) \tag{32b}$$

$$\dot{\theta}_{C1} + \dot{\theta}_{C2} = \omega''_{6C} + \omega''_{6'C} - \frac{2}{\gamma}(\dot{\psi} - \dot{\psi}_C) \tag{32c}$$

Substituting eqs.(25a), (26a), (27a) into eqs.(32a), (32b), (32c) leads to

$$\dot{\psi}_A(1 - \frac{2\rho}{\gamma}) + \frac{2\rho\dot{\psi}}{\gamma} = \rho(\omega''_{6A} + \omega''_{6'A}) \tag{33a}$$

$$\dot{\psi}_B(1-\frac{2\rho}{\gamma})+\frac{2\rho\dot{\psi}}{\gamma}=\rho(\omega''_{6B}+\omega''_{6'B}) \tag{33b}$$

$$\dot{\psi}_C(1-\frac{2\rho}{\gamma})+\frac{2\rho\dot{\psi}}{\gamma}=\rho(\omega''_{6C}+\omega''_{6'C}) \tag{33c}$$

From eqs.(31a), (31b), (31c) and eqs.(33a), (33b), (33c), we obtain the kinematic relations between the system input $\mathbf{u}$ and the system output $\mathbf{t}$, as shown below:

$$\mathbf{Ju}=\mathbf{Kt} \tag{34}$$

where $\mathbf{u}$ and $\mathbf{t}$ are both 6-dimensional vectors, while $\mathbf{K}$ and $\mathbf{J}$ are both 9×6 matrices, namely,

$$\mathbf{u}=\begin{bmatrix}\omega''_{6A}\\ \omega''_{6'A}\\ \omega''_{6B}\\ \omega''_{6'B}\\ \omega''_{6C}\\ \omega''_{6'C}\end{bmatrix},\qquad \mathbf{t}=\begin{bmatrix}\mathbf{t}_p\\ \dot{\psi}_A\\ \dot{\psi}_B\\ \dot{\psi}_C\end{bmatrix}, \tag{35a}$$

$$\mathbf{K}=\begin{bmatrix}\mathbf{h}_A & \mathbf{1}_2 & \mathbf{0}_2 & \mathbf{0}_2 & \mathbf{0}_2\\ \mathbf{h}_B & \mathbf{1}_2 & \mathbf{0}_2 & \mathbf{0}_2 & \mathbf{0}_2\\ \mathbf{h}_C & \mathbf{1}_2 & \mathbf{0}_2 & \mathbf{0}_2 & \mathbf{0}_2\\ 2\rho/\gamma & \mathbf{0}_2{}^T & 1-2\rho/\gamma & \mathbf{0}_2 & \mathbf{0}_2\\ 2\rho/\gamma & \mathbf{0}_2{}^T & \mathbf{0}_2 & 1-2\rho/\gamma & \mathbf{0}_2\\ 2\rho/\gamma & \mathbf{0}_2{}^T & \mathbf{0}_2 & \mathbf{0}_2 & 1-2\rho/\gamma\end{bmatrix}, \tag{35b}$$

$$\mathbf{J} = \begin{bmatrix} (r/2)\mathbf{j}_A & -(r/2)\mathbf{j}_A & \mathbf{0}_2 & \mathbf{0}_2 & \mathbf{0}_2 & \mathbf{0}_2 \\ \mathbf{0}_2 & \mathbf{0}_2 & (r/2)\mathbf{j}_B & -(r/2)\mathbf{j}_B & \mathbf{0}_2 & \mathbf{0}_2 \\ \mathbf{0}_2 & \mathbf{0}_2 & \mathbf{0}_2 & \mathbf{0}_2 & (r/2)\mathbf{j}_C & -(r/2)\mathbf{j}_C \\ \rho & \rho & 0 & 0 & 0 & 0 \\ 0 & 0 & \rho & \rho & 0 & 0 \\ 0 & 0 & 0 & 0 & \rho & \rho \end{bmatrix} \tag{35c}$$

where $\mathbf{0}_2$ represents the 2-dimensional zero vector and $\mathbf{1}_2$ the 2×2 identity matrix. Matrices $\mathbf{K}$ and $\mathbf{J}$ are, respectively, the forward and inverse Jacobian matrices of the WMR at hand, thereby completing the kinematic analysis of the WMR with three dual-wheel transmission units.

3.3 Mobility of a WMR with Three DWT units

With regard to our work on WMR, mobility refers to the number of independent generalized velocities that can be freely assigned without violating the kinematic constraints [8]. In our case, the kinematics of a WMR with three dual-wheel transmission units is derived in the form of eq.(34), which can be rearranged as

$$\mathbf{F}\dot{\mathbf{q}} = \mathbf{0} \tag{36}$$

where $\mathbf{0}$ denotes 9-dimensional zero vector, while the 9×12 matrix $\mathbf{F}$ and 12-dimensional vector $\dot{\mathbf{q}}$ are given below:

$$\mathbf{F} = \begin{bmatrix} \mathbf{K} & -\mathbf{J} \end{bmatrix}, \qquad \dot{\mathbf{q}} = \begin{bmatrix} \mathbf{t} \\ \\ \mathbf{u} \end{bmatrix} \tag{37}$$

Matrix $\mathbf{F}$ was termed by Freudenstein [9] the *functional matrix*. The vector $\dot{\mathbf{q}}$ of the generalized velocities comprising an excess of components over the mobility of the WMR, it is constrainted by eq.(36) to lie in the nullspace of $\mathbf{F}$, denoted by $\mathcal{N}(\mathbf{F})$. The dimension of nullspace of matrix $\mathbf{F}$ thus reveals the number of independent variables of the system. This number is therefore given by the nullity ν of $\mathbf{F}$, i.e.,

$$\nu = \dim[\mathcal{N}(\mathbf{F})]$$

In our case, matrix $\mathbf{F}$ has full row rank, i.e., $\text{rank}(\mathbf{F}) = 9$, and hence, $\nu(\mathbf{F}) = 3$. Thus, the WMR has a mobility of three, i.e., the number of velocities that we can freely specify is exactly three. Therefore, the WMR at hand has full mobility, i.e., it is omnidirectional. Once the independent velocities are specified, the remaining velocities can be derived uniquely from eq.(34).

3.4 The Isotropic Design of the WMR

A fundamental problem in robotics consists in determining the twist of a link of interest when the joint rates are given, or vice versa. The former is known as the *forward kinematics* problem, the latter as the *inverse kinematics* problem. The accuracy of the inverse and the forward kinematics of rolling robots depends on the *condition number* of the Jabobian matrices $\mathbf{K}$ and $\mathbf{J}$, whose inverses are required in the transformation from joint rates to platform twist and vice versa. For instance, if a robot is assigned to move in a desired trajectory, its joint variables and the time derivatives of these are calculated from inverse kinematics [10].

The condition number of a matrix is a measure of the relative roundoff-error amplification of the computed results with respect to the relative roundoff error of the input data, upon solving a system of equations associated with that matrix [12]. Hence, the accurary of the kinematic transformations depends on the condition number of the matrices whose inverses are needed. Matrices with small condition numbers produce accurate results, whereas matrices with large condition numbers produce results with correspondingly large roundoff errors. In fact, a condition number equal to unity, which does not introduce any roundoff-error amplification in the computations, is the best that can be achieved. Thus, robustness of the kinematic control is ensured when inverting a matrix with a condition number of unity. Matrices with such a condition number are called *isotropic* [11]. The condition number based on the Euclidean norm, denoted by κ, of an $m \times n$ matrix $\mathbf{A}$ can be defined as

$$\kappa \equiv \frac{\sigma_l}{\sigma_s} \tag{38}$$

where σ_l and σ_s are the largest and the smallest of the singular values of $\mathbf{A}$. Thus, singular matrices with $\sigma_s = 0$ have an infinitely large condition number, while isotropic matrices have all their singular values identical, and hence, $\sigma_s = \sigma_l$. Thus, κ is bounded from below and unbounded from above:

$$1 \leq \kappa < \infty \tag{39}$$

From the above discussion, it follows that an $m \times n$ isotropic matrix $\mathbf{A}$, with $m < n$, when multiplied by its transpose, produces a matrix that is a multiple of the $m \times m$ identity

matrix. Likewise, if $m > n$ in the above isotropic matrix $\mathbf{A}$, then the product of $\mathbf{A}^T\mathbf{A}$ is a multiple of the $n \times n$ identity matrix [11]. Apparently, we need to verify whether the two Jacobian matrices involved in our WMR can be rendered isotropic by design. We do this in the balance of this section.

Isotropy of J

In attempting to render $\mathbf{J}$ isotropic, we face a fundamental problem of incompatible units. Apparently, ρ is dimensionless, while $\mathbf{j}_A$, $\mathbf{j}_B$ and $\mathbf{j}_C$ are unit vectors and r has a unit of length. As a consequence, some singular values of $\mathbf{J}$ have unit of length and others are dimensionless, thus making it impossible to order them of $\mathbf{J}$ from smallest to largest. To overcome this problem, we introduce a *characteristic length* L, as suggested in [10]. Thus, we define $\mathbf{J}_L$ associated with L as

$$\mathbf{J}_L = \begin{bmatrix} (r/2L)\mathbf{j}_A & -(r/2L)\mathbf{j}_A & \mathbf{0}_2 & \mathbf{0}_2 & \mathbf{0}_2 & \mathbf{0}_2 \\ \mathbf{0}_2 & \mathbf{0}_2 & (r/2L)\mathbf{j}_B & -(r/2L)\mathbf{j}_B & \mathbf{0}_2 & \mathbf{0}_2 \\ \mathbf{0}_2 & \mathbf{0}_2 & \mathbf{0}_2 & \mathbf{0}_2 & (r/2L)\mathbf{j}_C & -(r/2L)\mathbf{j}_C \\ \rho & \rho & 0 & 0 & 0 & 0 \\ 0 & 0 & \rho & \rho & 0 & 0 \\ 0 & 0 & 0 & 0 & \rho & \rho \end{bmatrix} \tag{40}$$

Likewise, we define $\mathbf{u}_L$ associated with L as

$$\mathbf{u}_L = \begin{bmatrix} \omega''_{6A}L & \omega''_{6'A}L & \omega''_{6B}L & \omega''_{6'B}L & \omega''_{6C}L & \omega''_{6'C}L \end{bmatrix}^T \tag{41}$$

Then, L becomes an additional design variable, to be determined in order to either render the dimensionally homogeneous matrix $\mathbf{J}_L$ isotropic or minimize its condition number. To render $\mathbf{J}_L$ isotropic, the product $\mathbf{J}_L^T\mathbf{J}_L$ should be proportional to the 6×6 identity matrix. This product is

$$\mathbf{J}_L^T\mathbf{J}_L = \begin{bmatrix} \alpha+\beta & -\alpha+\beta & 0 & 0 & 0 & 0 \\ -\alpha+\beta & \alpha+\beta & 0 & 0 & 0 & 0 \\ 0 & 0 & \alpha+\beta & -\alpha+\beta & 0 & 0 \\ 0 & 0 & -\alpha+\beta & \alpha+\beta & 0 & 0 \\ 0 & 0 & 0 & 0 & \alpha+\beta & -\alpha+\beta \\ 0 & 0 & 0 & 0 & -\alpha+\beta & \alpha+\beta \end{bmatrix} \tag{42a}$$

where

$$\alpha \equiv \frac{r^2}{4L^2}, \qquad \beta \equiv \rho^2 \tag{42b}$$

To render $\mathbf{J}_L$ isotropic, it is obvious that we need $L = l/2$, such that

$$\mathbf{J}_L^T\mathbf{J}_L = \frac{2r^2}{l^2}\mathbf{1} \tag{43}$$

where $\mathbf{1}$ is the 6×6 identity matrix. The inverse kinematics of a WMR with three dual-wheel tranmission and isotropic $\mathbf{J}_L$ Jacobian is, then,

$$\mathbf{u} = \frac{l^2}{2r^2}\mathbf{J}_L^T\mathbf{K}\mathbf{t} \tag{44}$$

which does not require any matrix inversion and hence, $\mathbf{u}$ can be computed without any roundoff-error amplification.

Isotropy of K

Notice that introducing the characteristic length L has left unchanged the left-hand side of the first scalar equations of eq.(34), but has resulted in the same side of the last three equations multified by L, which requires that the corresponding right-hand side be multiplied by the same length. We also notice that γ and ρ are dimensionless, while $\mathbf{h}_A$, $\mathbf{h}_B$ and $\mathbf{h}_C$ have units of length. We thus need to introduce the *characteristic length* L again to overcome the dimensional incompatibility problem and to balance the last three equations of eq.(34). Thus, we define $\mathbf{K}_L$ and $\mathbf{t}_L$ associated with L as

$$\mathbf{K}_L = \begin{bmatrix} (1/L)\mathbf{h}_A & \mathbf{1}_2 & \mathbf{0}_2 & \mathbf{0}_2 & \mathbf{0}_2 \\ (1/L)\mathbf{h}_B & \mathbf{1}_2 & \mathbf{0}_2 & \mathbf{0}_2 & \mathbf{0}_2 \\ (1/L)\mathbf{h}_C & \mathbf{1}_2 & \mathbf{0}_2 & \mathbf{0}_2 & \mathbf{0}_2 \\ 2\rho/\gamma & \mathbf{0}_2{}^T & 1-2\rho/\gamma & \mathbf{0}_2 & \mathbf{0}_2 \\ 2\rho/\gamma & \mathbf{0}_2{}^T & \mathbf{0}_2 & 1-2\rho/\gamma & \mathbf{0}_2 \\ 2\rho/\gamma & \mathbf{0_2}^T & \mathbf{0}_2 & \mathbf{0}_2 & 1-2\rho/\gamma \end{bmatrix}, \qquad \mathbf{t}_L = \begin{bmatrix} \dot{\psi}L \\ \dot{\mathbf{c}} \\ \dot{\psi}_A L \\ \dot{\psi}_B L \\ \dot{\psi}_C L \end{bmatrix} \quad (45)$$

We thus substitute the characteristic length $L = l/2$ into the direct kinematics Jacobian $\mathbf{K}_L$. Moreover, for reasons of stability, balancing and symmetry, the three DWT units are to be mounted at the vertices of an equilateral triangle.

We thus have $\mathbf{h}_B = \mathbf{Q}\mathbf{h}_A$, $\mathbf{h}_C = \mathbf{Q}^T\mathbf{h}_A$ with denoting a 2×2 matrix rotating vectors in

the plane through an angle of 120°, or $2\pi/3$ rad. This matrix is given below:

$$\mathbf{Q} = \begin{bmatrix} \cos(2\pi/3) & -\sin(2\pi/3) \\ \sin(2\pi/3) & \cos(2\pi/3) \end{bmatrix}$$

Substituting the above conditions into $\mathbf{K}_L^T\mathbf{K}_L$, we obtain

$$\mathbf{K}_L^T\mathbf{K}_L = \begin{bmatrix} 3k^2+12\lambda^2 & 0 & 0 & k(1-k) & k(1-k) & k(1-k) \\ 0 & 3 & 0 & 0 & 0 & 0 \\ 0 & 0 & 3 & 0 & 0 & 0 \\ k(1-k) & 0 & 0 & (1-k)^2 & 0 & 0 \\ k(1-k) & 0 & 0 & 0 & (1-k)^2 & 0 \\ k(1-k) & 0 & 0 & 0 & 0 & (1-k)^2 \end{bmatrix} \tag{46}$$

where $k = 2\rho/\gamma$ and $\lambda = \|\mathbf{h}_A\|/l = d/l$, with $\|\mathbf{h}_A\|$ being the Euclidean norm of vector $\mathbf{h}_A$, which is nothing but the magnitude of $\mathbf{d}_j$, as shown in Fig. 5. We have thus assumed that all points P_j lie the same distance d from their centriod C.

We observe that $\mathbf{K}_L^T\mathbf{K}_L$ can not be rendered isotropic , since it can not be made proportional the identity matrix under any circumstances. We should thus try to minimize the condition number of the Jacobian matrix $\mathbf{K}_L$ over the design parameters k and λ.

The condition number of $\mathbf{K}_L$ is related to that of $\mathbf{K}_L^T\mathbf{K}_L$ by

$$\kappa(\mathbf{K}_L^T\mathbf{K}_L) = \kappa^2(\mathbf{K}_L) \tag{47}$$

Design Parameters	N_1	N_6	γ	r(mm)	l(mm)	ρ	k	d(mm)	λ
Value	25	20	0.8	92.0	154.0	0.6	1.5	154.0	1.0

Table 1: Design parameters of the WMR

Letting $\tilde{\mathbf{K}} \equiv \mathbf{K}_L^T \mathbf{K}_L$, the condition number $\kappa(\tilde{\mathbf{K}})$ is given by [12]

$$\kappa(\tilde{\mathbf{K}}) = \|\tilde{\mathbf{K}}\| \|\tilde{\mathbf{K}}^{-1}\| \tag{48}$$

If we use the weighted Frobenius norm [12] to define the condition number, we obtain

$$\|\tilde{\mathbf{K}}\|_F = \sqrt{\frac{1}{6}\mathrm{tr}(\tilde{\mathbf{K}}\tilde{\mathbf{K}}^{\mathrm{T}})} \tag{49}$$

where $\mathrm{tr}(\cdot)$ indicates the trace of $(\cdot)$. In our case, we have

$$\|\tilde{\mathbf{K}}\|_F = \sqrt{\frac{1}{6}\mathrm{tr}(\tilde{\mathbf{K}}^2)} \tag{50}$$

Likewise,

$$\|\tilde{\mathbf{K}}^{-1}\|_F = \sqrt{\frac{1}{6}\mathrm{tr}(\tilde{\mathbf{K}}^{-1}(\tilde{\mathbf{K}}^{-1})^{\mathrm{T}})} = \sqrt{\frac{1}{6}\mathrm{tr}((\tilde{\mathbf{K}}^{-1})^2)} \tag{51}$$

Since $\kappa(\mathbf{K}_L)$ is unbounded from above, we plot $1/\kappa(\mathbf{k}_L)$ in Fig. 7 vs. the design parameters k and λ. We notice that when $k = 1$, $1/\kappa$ vanishes, which means that κ tends to infinity, thus indicating, in turn, a rank-deficient $\mathbf{K}_L$.

Under the criterion of kinetostatic robustness [13] and using practical design values, the design parameters have been chosen as shown in Table 1. From Fig. 7, it seems that

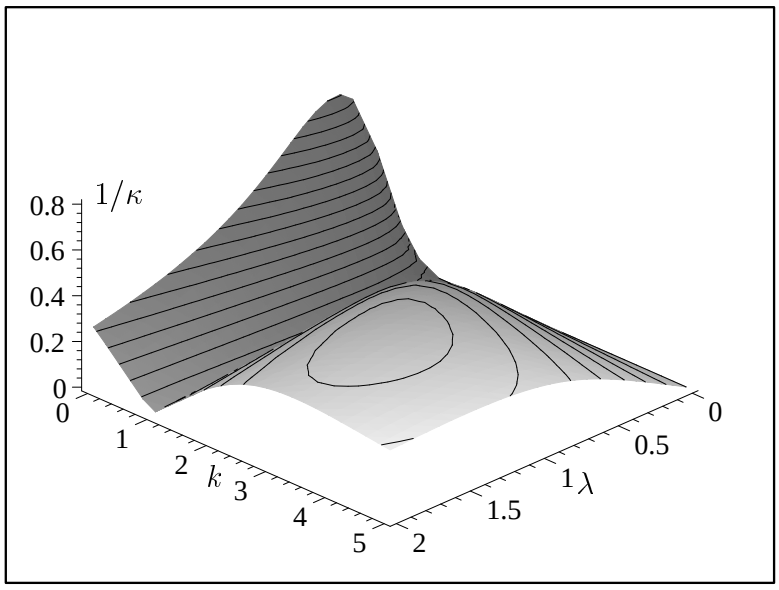

Figure 7: Condition number of Jacobian matrix $\mathbf{K}$

the minimum condition number of $\mathbf{K}$ occurs when $k = 0$ and $\lambda \approx 0.5$. However, from the Pythagorean Theorem, d is bounded as

$$d > \sqrt{\left(\frac{l}{2}\right)^2 + r^2}$$

which can be rewritten as

$$\lambda > \sqrt{\frac{1}{4} + \rho^2} \tag{52}$$

If r and l are defined as shown in Table 1 and the gear ratio γ is considered to be not greater than 1, we obtain $k = 2\rho/\gamma \geq 1.2$; from eq.(52) we obtain $\lambda \geq 0.79$.

Our design parameters shown in Table 1 are in the range of kinetostatic robustness and practical design.

3.5 Analysis of Simple Manoeuvres

We have just completed both the kinematic analysis of the WMR with three DWT units and the isotropic design of the WMR. We consider now three cases of simple manouvres of the WMR.

Case I

Shown in Fig. 8 is a WMR with three DWT units rotating about their steering axes, with the WMR remaining stationary. From eq.(34), we observe that if the output velocities of the two motors for each wheel unit are identical, i.e., if

$$\omega''_{6A} = \omega''_{6'A}, \qquad \omega''_{6B} = \omega''_{6'B}, \qquad \omega''_{6C} = \omega''_{6'C},$$

then the platform will remain stationary:

$$\dot{\psi} = 0, \qquad \dot{\mathbf{c}} = \mathbf{0}$$

Case II

The WMR performs a pure translation, in which the body orientation remains unchanged. We define two kinds of translation: *rectilinear translation*, in which all points of the platform move in parallel straight lines and *curvilinear translation*, in which all points move along congruent curves, as shown in Fig. 9.

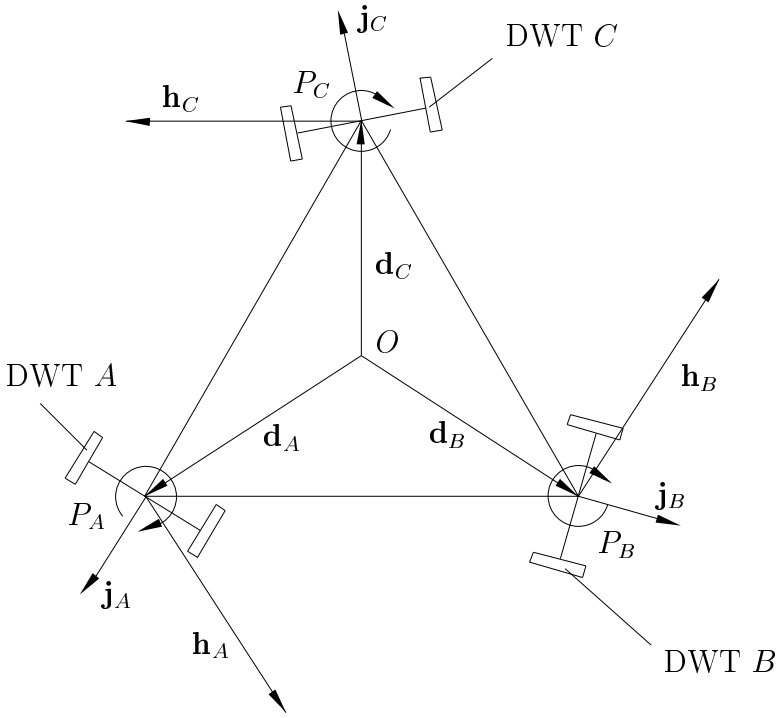

Figure 8: Reorientation of DWT axles, with stationary platform

In this case,

$$\dot{\psi} = 0, \qquad \dot{\mathbf{p}}_A = \dot{\mathbf{p}}_B = \dot{\mathbf{p}}_C = \dot{\mathbf{c}}, \qquad \dot{\psi}_A = \dot{\psi}_B = \dot{\psi}_C$$

From eqs.(31a), (31b) and (31c), we obtain

$$\omega''_{6A} - \omega''_{6'A} = \omega''_{6B} - \omega''_{6'B} = \omega''_{6C} - \omega''_{6'C} \tag{53}$$

From eqs.(33a), (33b), (33c), moreover,

$$\omega''_{6A} + \omega''_{6'A} = \omega''_{6B} + \omega''_{6'B} = \omega''_{6C} + \omega''_{6'C} \tag{54}$$

Combining eq.(53) and eq.(54), in turn, yields

$$\omega''_{6A} = \omega''_{6B} = \omega''_{6C}, \qquad \omega''_{6'A} = \omega''_{6'B} = \omega''_{6'C}$$

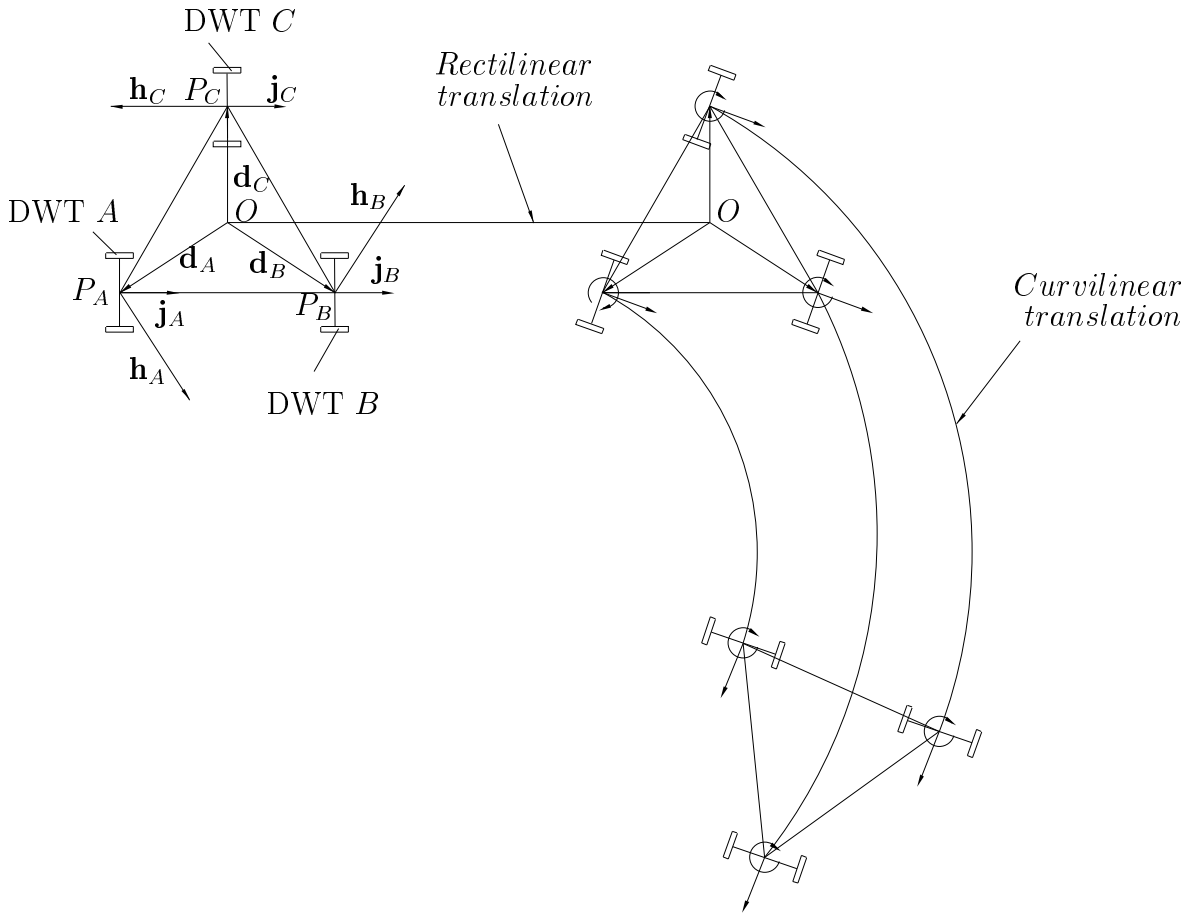

Figure 9: WMR under rectilinear and curvilinear translations

Case III

Shown in Fig. 10 is the WMR performing a pure rotation. The instant centre is selected as an arbitrary point K. Moreover, $a = \overline{P_A K}$, $b = \overline{P_B K}$ and $c = \overline{P_C K}$. We have

$$\frac{\dot{\mathbf{p}}_A}{a} = \frac{\dot{\mathbf{p}}_B}{b} = \frac{\dot{\mathbf{p}}_C}{c} = \dot{\psi}\mathbf{k}, \qquad \dot{\psi} = \dot{\psi}_A = \dot{\psi}_B = \dot{\psi}_C$$

where $\dot{\mathbf{p}}_A$, $\dot{\mathbf{p}}_B$, $\dot{\mathbf{p}}_C$ are the velocities of points P_A, P_B and P_C, respectively.

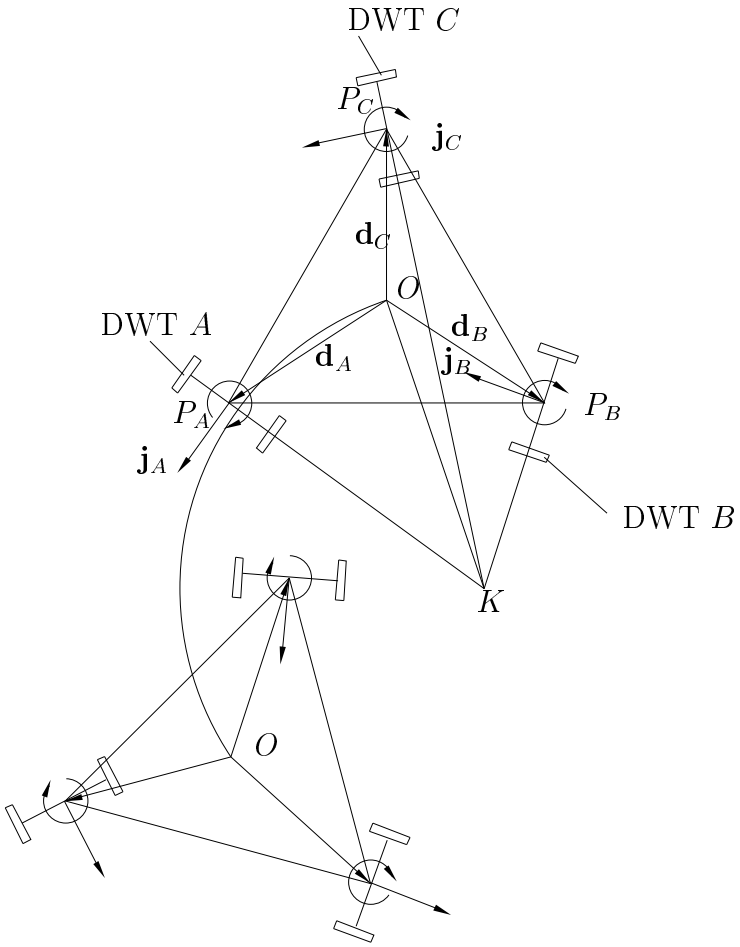

Figure 10: WMR under pure rotation about point K

From eqs.(25b), (26b), (27b) and eqs.(30a), (30b), (30c), we obtain

$$\dot{\psi} = \frac{r}{2a}(\omega''_{6A} - \omega''_{6'A}) = \frac{r}{2b}(\omega''_{6A} - \omega''_{6'A}) = \frac{r}{2c}(\omega''_{6A} - \omega''_{6'A}) \tag{55}$$

while eqs.(33a), (33b), (33c), yield

$$\omega''_{6A} + \omega''_{6'A} = \omega''_{6B} + \omega''_{6'B} = \omega''_{6C} + \omega''_{6'C}, \quad \dot{\psi} = \frac{r}{l}(\omega''_{6A} + \omega''_{6'A}) \tag{56}$$

From eq.(55) and eq.(56), in turn,

$$\omega''_{6A} + \omega''_{6'A} = \omega''_{6B} + \omega''_{6'B} = \omega''_{6C} + \omega''_{6'C}$$
$$= \frac{l}{2a}(\omega''_{6A} - \omega''_{6'A}) = \frac{l}{2b}(\omega''_{6B} - \omega''_{6'B}) = \frac{l}{2c}(\omega''_{6C} - \omega''_{6'C})$$

4 Mechanical Design of the Dual-wheel Mechanism

4.1 Design Specifications

The design specifications of the WMR with three DWT are:

Weight without batteries (one wheel unit): 40kg

Weight without batteries (WMR with three units): 120kg

Maximum payload: 280kg

Maximum speed: 1.5m/s

Maximum acceleration: 2m/s^2

Each DWT unit thus carries at least one-third of the total payload and the velocity and acceleration requirements remain as specified above.

4.2 Design Philosophy

The overall machine design process, involving multibody mechanical systems, can be broken down into two stages, namely, *kinematic design* and *mechanical design* [14]. Kinematic design comprises, in turn, three synthesis steps, namely, *type synthesis*, *number synthesis* and *dimensional synthesis* [15]. Type synthesis consists in finding which kind of mechanism, e.g., linkages, chains, gears or cams, is used to transmit motion and force. Number synthesis pertains to defining the number of mechanical components to be used. Dimensional synthesis aims at determining the geometric parameters of the mechanical system under design. For the WMR with three DWT units, the kinematic design was introduced in the previous section. For the mechanical design, the process involves materials, drive and control system selection. Mechanical design is essentially an iterative process [16]. We have completed the final iteration of the mechanical design of the WMR prototype, which was implemented in the CAD software system Pro-Engineer, as shown in Fig. 11.

Materials Selection

Since our WMR is to carry maximum loads of 280kg, the material of the drive shafts, gearhead shafts and motor output shafts must have enough strength. As the WMR is a research robot, some unpredictable incidents may occur. Thus, safety is our main criterion for the material selection of the shafts. Of carbon steels, AISI 4340 is a good choice for the material of the shafts under heavy-duty operation. Thus, AISI 4340 is our choice for the shafts of the WMR.

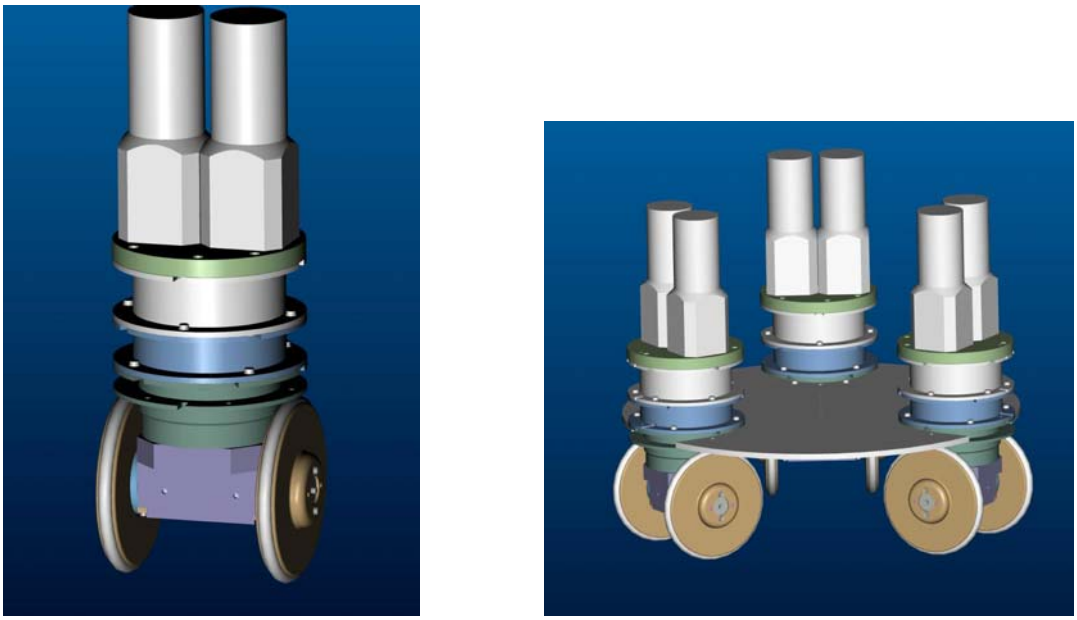

(a) (b)

Figure 11: Prototypes produced with Pro-Enigneer: (a) DWT unit (b) WMR with three DWT units

One of the important design considerations for the WMR is its size. In order to make it compact, novel needle roller bearings [17] are used between the hollow shaft mounted on gear 1 and the inner shaft mounted on gear 4, these gears being shown in Fig. 3. The inner shaft and the hollow shaft require case-hardening heat treatment by means of induction hardening [18].

Gear steels may be divided into two general classes, whether fabricated of plain carbon

steel or of alloy steel. Alloy steels are used to some extent in some industrial applications, but heat-treated plain carbon steels are far more common [18]. For most applications, plain carbon steels are satisfactory and quite economical. Through the assessment of gear load capacities, carbon steel AISI 4140 with induction-hardening treatment (52RC min) can satisfy our requirements for the gears. AISI 8620 is also a good choice, but the normal method of treatment is carburizing, which is much more expensive than the previous one.

Aluminium alloy is our choice for the material of the cases, covers and wheels. This material has the following properties [18]:

- light in weight, when compared with steel, brass or copper;
- highly machinable, when compared with composites;
- good stiffness properties;
- readily accepts a wide range of surface finishes and resists corrosion;
- avaliable in a wide range of sizes, shapes and forms.

One of the most versatile of the heat-treatable aluminium alloys, 6061-T6, is our choice.

Drive Selection

Gears

Helical gears are used in the double epicyclic mechanism of the WMR. Compared with standard spur gears, helical gears have the following important advantages [19]:

- Tooth strength is improved because of the elongated helical wraparound tooth base support;
- Contact ratio is increased due to the axial tooth overlap. Helical gears thus tend to have greater load-carrying capacity than spur gears of the same size. Noise can be largely decreased by using helical gears.
- Lower friction losses than spur gears, for contact point coincides with pitch point.

Motor

Electric motors come in all shapes and sizes. Electromagnetic direct current (DC) motors and electromagnetic alternating current (AC) motors are widely used. AC motors are typically used for heavy-duty machinery, such as machine tools, and are powered from an AC powerline. AC motors are seldom used in mobile robots because a mobile robot power supply is typically a DC battery [20]. As our WMR is a research robot, one may assume that the operation will be intermittent rather than continous, the extra maintenance required by DC motors thus being negligible. In addition, AC motors require costly and complex frequency control. DC motors are thus our choice for the WMR.

Characteristic	Stepper motor	DC motor
Continuous torque	High	Low
Peak torque	Limited	Very high
Torque ripple	Very high	Small
Power rate	Very high	High
Angular precision	Depends on the motor, not necessarily on number of steps/rev	Depends on the encoder resolution and severe-loop gain

Table 2: Stepper motor vs. DC motor

Another type of DC motors are stepper motors. Stepper motors are incremental motors powered by electrical pulses or steps. Table 2 [14] provides comparisons with characteristics between stepper motors and DC motors. From Table 2, although stepper motors have a higher continous torque than DC motors, the peak torque, which is important in robotics, is greater for DC motors. Moreover, the torque ripple for DC motors is less than that for stepper motors, which is important for low-speed robot operation. DC motors are commonly used for smaller jobs and will suit our requirements well.

A DC motor usually runs at high speeds, of the order of krpm, and has a too low torque to drive the wheel loads, the motors thus needing gearheads. It can be concluded that DC gearhead motors would best meet our WMR power requirements.

Control System Selection

The control system of the WMR will include a host computer, a motion controller, a power amplifer, DC gearhead motors and position sensors. Here we discuss only the selection of the position sensors.

One way to measure wheel angular displacement, and to synchronize the velocity of the two wheels is to connect an encoder to each motor shaft [20]. Typically, a shaft encoder is mounted on the output shaft of a drive motor or an axle. There are two types of shaft encoders, namely, absolute and relative, or incremental. For absolute encoders, the signal delivered by them is a code that corresponds to a particular orentation of the shaft. For relative incremental encoders, the signal delivered is a pulse train. The latter can be divided into one- and two-channel types. Absolute encoder operation needs more electronics equipment and space, which makes them larger than the equivalent two-channnel encoders [14]. Although one-channel incremental encoders are small, their resolution is significantly lower than those of two-channel encoders. By far, two-channel incremental encoders are the most widely used optical encoders. Incremental two-channel encoders are our choice for the WMR, as they can be purchased as enclosed units or built-in as an integral part of the drive motor.

4.3 Bill of Materials for the DWT

We can divide the whole assembly of the DWT into three parts:

- Wheel sub-assembly;
- Transmission sub-assembly;
- Case sub-assembly

The bill of Materials for the three sub-assemblies is listed in Tables 1, 2 and 3 of the Appendix.

4.4 Manufacturing Drawings

A complete set of manufacturing drawings was produced. These drawings, totally 31, are not included here to keep the size reasonable. The drawings are available in [21].

5 Conclusions

The kinematics, mobility analysis and design of a wheeled mobile robot with three dual-wheel transmission units were discussed.

Regarding the kinematics of the WMR, we first formulated the kinematic relations of one DWT unit. Next, the kinematics of the whole WMR with three DWT units was derived.

We also studied the mobility of the WMR with three DWT units. The functional matrix was introduced to analyze the mobility of the WMR. We demonstrated that the WMR with three DWT units has a mobility of three. Therefore, the WMR at hand has full mobility; it is thus omnidirectional. Then, three cases of simple manoeuvres of the WMR were analyzed.

For design purposes, kinetostatic robustness was our main objective. We found that the WMR with three DWT units can not be rendered isotropic, and certain design parameters can cause singularities. This means that the singularity of the WMR depends not only on the motions of each DWT unit with respect to the platform, but also on the design geometric parameter, specially $k = 2\rho/\gamma = 1$. Moreover, under the criterion of kinetostatic robustness and reasonable design, the values of design parameters of DWT units of the WMR have been chosen.

A novel dual-wheel transmission based on double epicyclic gear trains was designed. A prototype of the WMR with three dual-wheel transmission units using epicyclic cam mechanisms is in the works.

References

[1] Muir, P.F. and Neuman, C.P. 1987. Kinematic modeling of wheeled mobile robots. *J. Robotic Systems*, 4 (2): 281–340.

[2] Leow, Y.P. 2002. *Kinematic Modelling, Mobility Analysis and Design of Wheeled Mobile Robots*. M.Eng. Thesis, Nanyang Technological University, Singapore.

[3] Wada, M., Takagi, A. and Mori, S. 2000. Caster drive mechanisms for holnomic and omni-directional mobile platform with no cover constraint. *Proc. IEEE Int. Conf. Robotics and Automation*, pp. 1531–1538, San Francisco, California.

[4] Killough, S.M. and Pin, F.G. 1992. Design of an omnidirectional and holonomic wheeled platform prototype. *Proc. IEEE Int. Conf. Robotics and Automation*, pp. 84–90, Nice, France.

[5] Ferrière, L. and Raucent, B. 1998. Rollmobs, a new universal wheel concept. *Proc. Int. Conf. Field and Service Robotics*, pp. 1877–1882, Leuven, Belgium.

[6] Lynwander, Peter. 1983. *Gear Drive Systems*. Marcel Dekker, Inc. New York.

[7] Angeles, J. 2002. *Fundamentals of Robotic Mechanical Systems. Theory, Methods, and Algorithms*, Second Edition, Springer-Verlag, New York.

[8] Ostrovskaya, S. 2001. *Dynamics of Quasiholonomic and Nonholinomic Reconfigurable Rolling Robots*. Ph.D Thesis, McGill University, Montreal, Canada.

[9] Freudenstein, F. 1962. On the variety of motions generated by mechanisms. *ASME J. of Engineering for Industry*, 84: 156–160.

[10] Saha, S.K., Angeles, J. and Darcovich, J. 1995. The design of kinematically isotropic rolling robots with omnidirectional wheels. *Mechanism and Machine Theory*, 30 (8): 1127–1137.

[11] Strang, G. 1988. *Linear Algebra and Its Application*, Third Edition, Harcourt Brace Jovanovich College Publishers, New York.

[12] Golub, G. H. and Van Loan, C. F. 1983. *Matrix Computations*. Baltimore, Maryland: The Johns Hopkins University Press.

[13] Angeles, J. 2002. The robust design of parallel manipulators. *Proc. 1st International Colloquium Robotic Systems for Handling and Assembly*, pp. 9–30, Braunschweig, Germany, May 29–30.

[14] Williams, O. R., Angeles, J. and Bulca, F. 1993. Design Philosophy of an isotropic six-axis serial Manipulator. *Robotics and Computer-Integrated Manufacturing*, Vol. 10, No. 4, pp. 275–286.

[15] Hartenberg, R.S., Denavit, J. 1964. *Kinematic Synthesis of Linkage*. New York, McGraw-Hill.

[16] Ullman, David G. 1997. *The Mechanical Design Process*, Second Edition, McGraw-Hill, Boston, Massachusetts.

[17] Catalogue of Needle Roller Bearing. 2001. INA Inc.

[18] Oberg, E., Jones, F. D. and Horton, H. L. 1988. *Machinery's Handbook* 23rd Edition. Industrial Press Inc. New York.

[19] Stock Drive Products: *Handbook of Small Standardized Components, Master Catalog 757.* New Hyde Park, New York.

[20] Jones, Joseph L., 1999. *Mobile Robots Inspiration to Implementation.* A. k. Peters, Ltd. Wekkesley, Massachusetts.

[21] Tang, Fan., Angeles, J. 2002. *Kinematics and Design of a Wheeled Mobile Robot.* Department of Mechanical Engineering & Centre for Intelligent Machines Technical Report TR-CIM-02-13, McGill University, Montreal.